Am J Transl Res 2025;17(3):1662-1678
www.ajtr.org /ISSN:1943-8141/AJTR0160696

Original Article

Altered uterine artery protein signature and function following E-cigarette exposure in pregnancy

Alexander Juusela[1,2,4], Vishal D Naik[2], Alexander L Carabulea[2], Joseph D Janeski[2], Hong Jiang[2], Saravanan Venkatachalam[5], Jayanth Ramadoss[2,3]

[1]Department of Obstetrics and Gynecology, Division of Maternal-Fetal Medicine, Wayne State University School of Medicine, Detroit, Michigan, USA; [2]Department of Obstetrics and Gynecology, C.S. Mott Center for Human Growth and Development, School of Medicine, Wayne State University, Detroit, Michigan, USA; [3]Department of Physiology, School of Medicine, Wayne State University, Detroit, Michigan, USA; [4]Detroit Medical Center, Detroit, Michigan, USA; [5]Department of Industrial and Systems Engineering, Wayne State University, Detroit, Michigan, USA

Received September 23, 2024; Accepted January 26, 2025; Epub March 15, 2025; Published March 30, 2025

Abstract: Objective: Over the past decade e-cigarette (e-cig) usage has become a growing public health concern, especially during pregnancy as many perceive e-cigs as a safer alternative to combustible cigarettes. Although human and animal models exhibit altered uterine artery Doppler velocimetry and waveform abnormalities following traditional smoking and buccal nicotine exposure, the effects of e-cig aerosols on pregnancy are incompletely researched and understood. We hypothesized that an altered uterine artery proteomic signature, accompanied by functional deficits, will be caused by e-cig vaping during pregnancy. Methods: In a validated timed pregnant Sprague-Dawley rat model system, a custom-engineered vaping system comprising a commercial atomizer and vape unit was utilized to generate and deliver e-cig aerosols that mimic the aerosols produced by commercial e-cigs, once daily, to pregnant dams. Results: Mean fetal weight, crown-rump length, and placental weight were significantly lower in the E-Cig group than those in the pair-fed Control group. Mass spectrometry followed by proteomic analysis detected a total of 2129 proteins; 36 significantly altered proteins were mostly related to immune system and vasodilation. Principal component analysis validated the protein signature. The uterine arteries of e-cig exposed rats demonstrated impaired concentration-dependent acetylcholine-induced uterine artery relaxation. Supplementation of N(ω)-nitro-L-arginine methyl ester (L-NAME) confirmed a role for the nitric oxide (NO) system. Immunofluorescence validated the localization to the uterine artery endothelium and the decreased levels of vasodilatory excitatory P-Ser^{1177} endothelial NO synthase. Conclusions: Identifying the pathway(s) involved in the pathogenesis of uterine artery dysfunction creates a potential for pinpointing antagonistic and/or reversal medications, thereby preventing or reducing e-cigarette mediated uteroplacental dysfunction and fetal growth restriction.

Keywords: Gestation, E-cigarette, nicotine, vaping, maternal, fetal growth restriction, teratogen, uterine, vascular, pregnancy

Introduction

Nicotine usage in the United States was on a downward trajectory [1] until electronic cigarettes entered the market around 2007. Since then, an epidemic of e-cigarette (e-cig) usage has occurred in the United States, especially amongst adolescents and reproductive-aged persons. Driving this epidemic is the perception that e-cigs are a safer or less-harmful alternatives to traditional tobacco cigarette smoking [2-6], cheaper [5, 6], more flavorful [5, 6], and useful as effective smoking cessation aids [5, 6].

From 2000 to 2020, the proportion of persons who quit smoking during pregnancy significantly increased from 43.2% to 53.7%, respectively [7]. Despite this optimistic progress, approximately half of the persons who smoke prior to pregnancy remain at risk for exposure-related adverse pregnancy outcomes as they continue to smoke while pregnant and postpartum [7, 8]. The belief that e-cigarettes are a healthier substitute for traditional tobacco cigarettes still persists, despite public health campaigns. A 2017 point-prevalence survey found that 74.6% of pregnant e-cigarette users switched to e-cig-

https://doi.org/10.62347/KEWQ6629

arettes from traditional cigarettes when they learned they were pregnant [9].

Adverse perinatal outcomes secondary to nicotine smoking was first documented in the 1950's [10], when a dose-dependent association between the number of cigarettes smoked per day and prematurity rates was identified [10]. Since initial reports, studies have consistently demonstrated adverse perinatal outcomes including placental abruption, spontaneous preterm birth, fetal growth restriction (FGR) [11, 12], low birth weight (LBW) [11, 13], fetal and neonatal death [14]. An additional source of nicotine exposure, e-cig vaping during pregnancy is a risk factor for spontaneous preterm birth (PTB) [15], FGR [16], small for gestational age (SGA) [15], and low birth weight (LBW) [15], compared to non-tobacco (e-cig and traditional cigarette) smokers. However, there is no statistically significant difference in SGA, LBW, or PTB between e-cig and traditional tobacco smokers [15]. Albeit the known adverse perinatal outcomes, there exist major knowledge gaps regarding the maternal, fetal, neonatal, and long-term offspring effects of e-cigarette vaping during pregnancy. This highlights the importance of continued medical and translational research regarding the adverse pregnancy effects of e-cigarette vaping.

Impaired blood flow through the uterine arteries can lead to insufficient delivery of O_2 and nutrients to the fetus and is directly correlated with FGR [17]. We therefore hypothesized that E-cig vaping during pregnancy leads to fetal growth deficits that is accompanied by significant alterations to uterine artery protein signature profile. To date we are not aware of a single proteomic study in the E-cig field performed during pregnancy. We therefore performed a mass spectrometry analysis as the rapidly evolving field of proteomics holds great potential for developing advanced biomarkers capable of detecting subtle biological changes specifically linked to E-cig vaping. Based on these findings, and our previous studies that demonstrated E-cig-derived nicotine-mediated uterine and umbilical artery vascular Doppler velocimetry disruptions, we conducted studies to test downstream pathways to exam disruption in uterine artery function.

Methods and materials

The methods performed for the e-cig Vaping System and the Exposure Paradigm were performed as previously published by our group [18, 19].

Treatment groups

All experimental procedures were approved by the Institutional Animal Care and Use Committee at Wayne State University and in accordance with National Institutes of Health guidelines (NIH Publication No. 85-23, revised 1996). Commercially purchased, 6-7 weeks old, timed pregnant, Sprague-Dawley rats (Charles River, Wilmington, MA) were housed in individual cages with a 12:12-hour light-dark cycle and a temperature-controlled room (23°C). Rats were randomly assigned to one of two treatment groups: unexposed to vaping control (Control) and an exposed E-Cig group (E-cig) which were exposed to nicotine in an e-cig base liquid (Juice). The Juice was composed of 80:20 propylene glycol (Fisher) to glycerol (Acros Organics), a ratio designed to be similar to e-cig liquids commercially available in most vaping shops [20]. Prior to initiation of vaping, to control for nutritional intake throughout the study, Control rats were yoked with an E-Cig vaping animal of similar weight, and administered matched daily feed amounts. The Control group also served as a control for the vaping procedure. Control animals were housed in vaping chambers identical to those in the E-Cig groups for an equivalent duration, but with only room air passing through the chamber at a flow rate matching the vaping groups. The E-Cig group allowed for the testing of the effects of vaping e-cig liquid with nicotine, as a majority of e-cig consumers use devices containing e-cig liquid with nicotine.

E-cig vaping system

The inhalation chambers resembled the animal housing cages in that they were airtight, amber, polymer containers. A custom-engineered vaping chamber system with precision-controlled aerosol release technology was used to establish the e-cig vaping paradigm. This setup allowed for uniform delivery of a customized e-cig vapor profile to the vaping treatment group [18]. We utilized a Geekvape Zeus Subohm tank, Mesh Z2 coil at 0.2 ohm and matched via a programmable atomizer to a 60 W output source. The programmable atomizer apparatus produced equilibrated and uniform e-cig vapor plumes by vaporizing a standardized liquid volume per unit time [18], designed

to be equivalent to the latest generation of e-cig atomizers currently available to, and used by, the public. All subjects in the treatment group were exposed only to e-cig vapor dispensed under the control of the programmable atomizer. Voltage delivered to the programmable atomizer, puff duration, and puff frequency within the inhalation chamber were controlled by a sophisticated software interface. The software interface was unique in that it produced vape puff profiles identical to those produced by commercial e-cigs. Unidirectional silicone tubing (6 mm inner diameter, 10 mm outer diameter) with one-way exhaust valves directed airflow throughout the system. Prior to passing through facility exhaust ducts, all emissions from the inhalation chambers passed through activated charcoal filters to remove any harmful particles.

Exposure paradigm

As previously described, airflow through the chambers was maintained at a constant flow rate of 2.5 L/min, with a four second e-cig vapor puff dispensing approximately 42 mL puff volumes every 2 minutes. The puff duration was timed specifically to ensure proper ventilation of the chambers and removal of accumulating aerosols. The e-cig base liquid was compounded in-house at room temperature at a composition of 80:20 propylene glycol (Fisher) to glycerol (Acros Organics), a ratio similar to e-cig liquids bought in most vaping shops [20]. Due to the relative viscosities of propylene glycol and glycerol, this e-cig liquid ratio was preferred for our paradigm to maintain adequate absorption of e-cig liquid by the cotton wick. Recent studies on e-cig liquid composition have reported that propylene glycol-based liquids provide a higher nicotine delivery ratio than glycerol-based liquids [21]. The treatment group received e-cig base liquid with the addition of 5% (50 mg/mL) nicotine during acclimatization followed by 10% (100 mg/mL) nicotine. E-cig liquid nicotine concentration was based on our previous study in which rat E-cig aerosols and blood nicotine concentrations were characterized by mass spectrometry [18] and selected with consideration for the average nicotine concentration of commercially available e-cig liquids [22, 23]. Our previously published study demonstrated that this dosing system and paradigm resulted in a median peak serum nicotine concentration in dams = 27.7 ng/mL, comparable to moderate/high level human smokers [18]. The dams underwent twice daily vaping treatments of 1.5 hours each (3 hours of total exposure per day), five days a week, beginning on gestational day (GD) 5 until GD 20, prior to parturition [24].

Maternal, fetal, and placental weight measurements

Maternal weight (number of dams, Control, n = 16; E-cig, n = 16) was recorded on GD 21, one day after the last e-cig administration on GD 20. To assess the developmental implications of e-cig exposure on growth, crown-rump length, fetal body weight, and placental weight were measured for the fetuses. Dams were euthanized, the concepti were carefully extracted, and each placenta and fetus were separated and individually weighed. Fetal and placental weights were recorded. Fetuses from a subset of dams had crown-rump length measured and recorded. Litter size was analyzed for each dam.

Protein digestion and preparation

Uterine artery tissues (number of dams, Control, n = 5; E-Cig, n = 5) were solubilized and buffered by adding 2% lithium dodecyl sulfate (LiDS, Sigma L9781) in 20 mM tris buffer pH 8.0. Samples were homogenized in a Bullet Blender (Next Advance) using 3.2 mm stainless steel beads (SSB32, Next Advance) for 1 minute at setting 8. To deactivate enzymes, samples were heated for 5 minutes at 90°C. Samples were then reduced by adding 5 mM DL-dithiothretol (DTT, Sigma cat# D5545) and incubated 30 minutes at 37°C. Alkylation was performed by adding 15 mM Iodoacetamide (IAA, Sigma cat# I1149) and samples were incubated at room temperature for 30 minutes in the dark. The alkylation reaction was stopped by adding 5 mM DTT. Samples were centrifuged 10 minutes at 17,000 g to eliminate particulates and supernatants were transferred to new tubes. Samples were acidified by adding 10% of the original volume of 12% phosphoric acid, precipitated by adding 5 volumes of methanol (MeOH), followed by incubation overnight at -20°C. Tubes were centrifuged at 13,000 RPM for 10 minutes and pellets washed with 80% MeOH/1% TEAB. Washed pellets were allowed to dry on the bench then dispersed in a

buffer containing 20 mM Tris buffer pH 8.0/10 mM CaCl2/10% ACN. A protein assay (Pierce protein assay, cat#23225) and the tryptic digest of 100 µg proteins/samples was performed by adding a ratio of 1 µg trypsin per 20 µg proteins (Promega, V5113) per sample then incubating for 1 hour at 47°C followed by overnight incubation at 37°C.

Mass spectrometry analysis

Following LC/MS/MS to check for digestion miscleavages, a Thermo Vanquish Neo UHPLC chromatography system with an EasySpray source was used to perform final analysis. The trapping column was an Acclaim PepMap 100, 75 µm × 2 cm and the resolving column was an Ionopticks Aurora Ultimate, 75 µm × 25 cm, 1.7 µm C18. LC-MS/MS acquisition used a 120-minute gradient with Data Dependent Analysis on an Orbitrap Eclipse MS system. MS1 spectra were acquired at 120,000 resolution in the 350 to 1500 Da and MS2 were acquired in the ion trap with collision energy of 30% and maximum injection time of 50 msec.

Protein identification and quantification

Data analysis was conducted using Proteome Discoverer 2.5 Scaffold software 5.0 employing Sequest-HT and Percolator algorithms to search a rat database containing 8114 protein entries. The search parameters were allowed for up to 2 missed cleavages by trypsin digestion. Fixed modification included carbamidomethylation of cysteine, while dynamic modifications were deamination of asparagine and glutamine, oxidation of methionine as well as a dynamic N-terminus acetyl modification. A False Discovery Rate (FDR) was set at 0.01 for high confidence matches. Analysis files were imported into Scaffold 5.0 for data visualization.

Dimensionality reduction and clustering

Principal Component Analysis (PCA) was utilized to transform the significantly enriched proteins into low-dimensional uncorrelated components. The number of dominant uncorrelated components was deducted using cumulative explained variance. We then performed low-dimensional transformations for the Control and the E-cig groups and clustered using the k-means clustering algorithm. The parameter 'k' which denotes the ideal number of clusters was determined using Within-Cluster Sum of Square (WCSS); WCSS was calculated as the sum of the squared distance between each point and the centroid within a cluster. The number of clusters was determined using WCSS and the elbow method. Each Control and E-cig's PCA component was assigned to a cluster based on the corresponding centroids of the clusters.

Endothelial-mediated vasodilation of the uterine artery

Functional uterine artery studies were conducted in a random set of yoked rats. Pregnant Control (n = 5) and E-Cig-administered (n = 5) rats were utilized to study the functional response as well as mechanistic studies of the primary uterine artery. As previously described [25], following euthanasia, whole uteruses were transferred to large 200 mm petri dishes containing ice-cold HEPES-bicarbonate solution, pH 7.4 (NaCl 130 mM; HEPES 10 mM; glucose 6 mM; KCl 4 mM; $CaCl_2$, 2.4 mM; EDTA 0.024 mM; KH_2PO_4 1.18 mM; $MgSO_4.7H_2O$ 2.5 mM; $NaHCO_3$ 4.05 mM) and pinned on solidified sylgard to facilitate uterine artery dissection. Approximately 3-5 mm segments of primary uterine artery were excised between bifurcations. Connective tissue and surrounding fat surrounding the segment were removed. Standard procedures for a dual-chamber pressure arteriograph system were employed as described previously. Cleaned arterial segments from each group were mounted onto a glass cannula connected to a pressure transducer and secured via two nylon ligatures in a dual-vessel arteriograph chamber. Residual blood was removed from the vessel lumen by gently passing ice-cold HEPES buffer through the glass cannula. The free vessel end was ligated and securely fastened to the opposing cannula with two nylon ligatures. Both chambers of the arteriograph were continuously circulated with pre-warmed HEPES buffer fixed at 37°C. Intraluminal pressure was maintained and monitored using pressure servo controllers and a pressure monitors, respectively. This setup advantageously permitted uniform experimental conditions for consecutive vessels from Control and e-cig-exposed dams to be studied. Following this, intraluminal pressure was increased to 60 mmHg, at which pressure

the vessel exhibited myogenic tone and then equilibrated for 1 hour (hr). After equilibration, intraluminal pressure was increased to 90 mmHg to mimic *in vivo*-like conditions, at which pressure all data were recorded using Ion Wizard 6.6 (IonOptix) software. Vessels were pre-contracted with 10^{-7} M thromboxane (Tbx) for 20 minutes (mins) or until vessel diameter stabilized. The Tbx concentration for the current study was determined using concentration response curve previously generated in our laboratory [26]. Tbx treatment was followed by administration of three-fold increasing doses of acetylcholine (Ach) from 10^{-10} M to 10^{-5} M, to obtain the corresponding dose response. Data were recorded for 3-5 min at each dose increments or until variable measurement remained constant.

Inhibition of nitric oxide-mediated vasodilation of the uterine artery

Following measurement of endothelium-mediated vasodilation, we measured the nitric oxide (NO)- mediated proportion of vascular relaxation. Endothelial cells produce NO by catalyzing L-arginine to L-citrulline. Once UA diameter remained constant following administration of Ach 10^{-5} M, blockade of NO vasodilatory pathways was performed by administering 10^{-4} M N(ω)-nitro-L-arginine methyl ester (L-NAME), an L-arginine analogue and NO inhibitor, which abolished the Ach-induced NO-component of relaxation in the rat uterine artery [27].

Immunofluorescence

Maternal uterine arteries from yoked pregnant Control and E-Cig rats were excised on GD 21, and carefully inserted in Tissue-Tek Optimal Cutting Temperature compound (OCT) (Sakura Finetek U.S.A., Inc.) before placing on dry ice to solidify. Solidified blocks were put in an air tight bag and stored at -80°C until sectioning. 8 µm segments were prepared using a Leica CM1860 cryostat (Leica Biosystems, Inc.), carefully transferred onto positively charged microscope slides. Slides were stored in a -80°C freezer until undergoing immunostaining. For staining, frozen sections were fixed sequentially with ice-cold methanol (30 min, -20°C) and 4% paraformaldehyde (30 minutes, 4°C), rinsed in phosphate-buffered saline (PBS), incubated in 10% normal goat serum (1 hr) to block unspecific binding, and incubated overnight (4°C) with either a primary antibody (1:200; P-Ser^{1177}eNOS; Cell Signaling Technology; #9571) or PBS (negative control) in a humidified chamber. The following day, the tissues were incubated in goat anti-mouse secondary or goat anti-rabbit antibody (1:250; IgG Alexa 488; Invitrogen; #A11008) at room temperature, in the dark, for 1 hr. After washing with PBS, 1 drop of anti-fade mounting media with DAPI (Invitrogen; #P36931) was applied to each slide, and coverslipped. Mounting medium was allowed to dry overnight. Slides were imaged the next day using an Olympus BX63 stereomicroscope and Olympus cellSense Dimension software (Olympus, Japan).

Statistics

Study variables (maternal, fetal, and placental weights as well as crown-rump length (CRL), litter size, and placental efficiency) were confirmed to be normally distributed using Kolmogorov and Smirnov tests. Comparisons were conducted between the Control and E-Cig groups. Pregnancy groups were compared by unpaired Student's t-test with the e-cig exposure as the sole independent variable. Comparisons between groups were considered statistically significant when the two-tailed $P < 0.05$. Data are reported in the text, figures, and tables as the mean ± standard error of the mean (SEM). A two-way repeated measures ANOVA was used to analyze vascular functional response data, with treatment group as the between factor and dose as the within factor, followed by analysis with Fisher's Least Significant Difference (LSD) multiple comparison test. GraphPad Prism (GraphPad Software, Inc.) was used to analyze the data, which are presented as mean ± SEM, with significance established at $P < 0.05$.

Results

Maternal, fetal and placental weight, as well as crown-rump length, and placental efficiency measurements are shown in **Table 1** and illustrated in **Figure 1**. There was no statistical difference in the maternal weight between the two groups prior to the start of the study or on GD 21 (Control, n = 16, mean 307.28 ± 7.57 g; E-Cig, n = 16, 293.07 ± 9.89 g; P = 0.263 [95% CI (-11.22-39.64)]. Litter size between groups was not significantly different (average litter size, Control = 11.25 ± 0.60, E-Cig = 10.69 ±

Table 1. Maternal and fetal characteristics at gestational day 21 of control and e-cig exposed groups

	Control	E-cig	*P* value (*P*)	95% Confidence Interval
Maternal Weight (g)	307.28±7.57	293.07±9.89	0.2629	-11.22-39.64
Fetal Weight (g)	3.31±0.20	2.67±0.188	0.0276	0.07-1.19
Placental Weight (g)	0.53±0.018	0.42±0.018	< 0.0001[a]	0.06-0.17
Placental Efficiency	6.262±0.39	6.3314±0.27	0.8836	0.89-1.03
Fetal CRL (mm)	37.92±1.56	33.02±0.98	0.0131[a]	1.12-8.69

Data are presented as mean ± standard error of the mean. Groups were compared by unpaired Student's t-test with the e-cig exposure as the sole independent variable. Comparisons between groups were considered significant when the two-tailed P < 0.05. GD, gestational day. Placental efficiency = fetal weight (g)/placental weight (g). [a]Statistically significant.

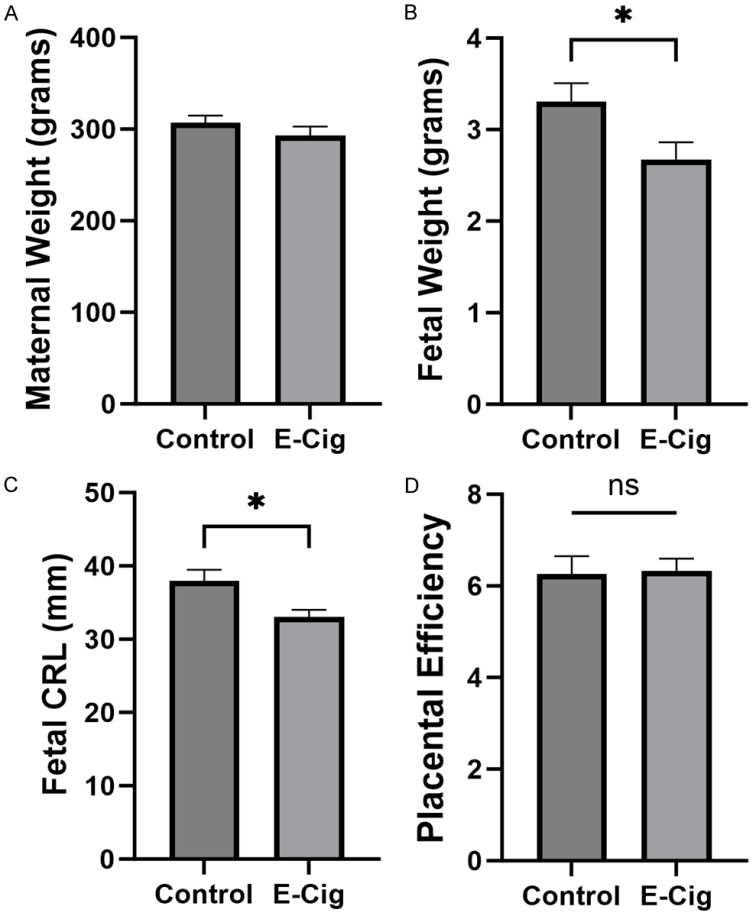

Figure 1. (A) Maternal weight, (B) fetal weight, (C) fetal crown-rump length, and (D) placental efficiency of controls and E-cig groups. Data are expressed as mean ± SEM. (*) represents statistical significance compared to controls. Significance was established *a priori* at P < 0.05. NS represents non-significant difference when compared to controls.

0.66, P = 0.5304). Mean fetal weight in the E-Cig group (mean 2.67 ± 0.19 g) was significantly decreased by 17.41% (unpaired Student's T-test, P = 0.028) compared to the Control group (mean 3.31 ± 0.20 g). Placental weight in the E-Cig group (mean 0.42 ± 0.02 g) was significantly decreased by 19.81% (unpaired Student's T-test P < 0.0001 compared to the Control group (mean 0.53 ± 0.02 g). Placental efficiency, an indirect measurement to calculate the efficiency by which the placenta transfers nutrients to the fetus [28] was not statistically different between the two groups (P = 0.884), and was calculated as fetal weight in grams divided by its respective placental weight in grams. Fetal crown-rump length measured in the E-Cig group (mean 33.02 ± 0.98 mm) was significantly decreased by 11.57% (unpaired Student's T-test P = 0.013] compared to the Control group (mean 37.92 ± 1.56 mm).

E-cig vaping significantly altered the protein signature profile

Mass spectrometry followed by proteomic analysis detected a total of 2129 proteins. Of these 37 proteins were significantly altered (**Figure 2**). Among the significantly altered proteins, the most abundant included fibronectin (Fn1, P = 0.023), immunoglobulin G2A (IgG2A, P = 0.032), and alpha-1-microglobulin (A1M, P = 0.016). Interestingly, all these proteins were glycosylated, indicating that e-cigs have a major effect on glycoproteins. Among other abundant proteins, plastin 3 (PLS3, P = 0.033), a protein that is S-nitrosylated and

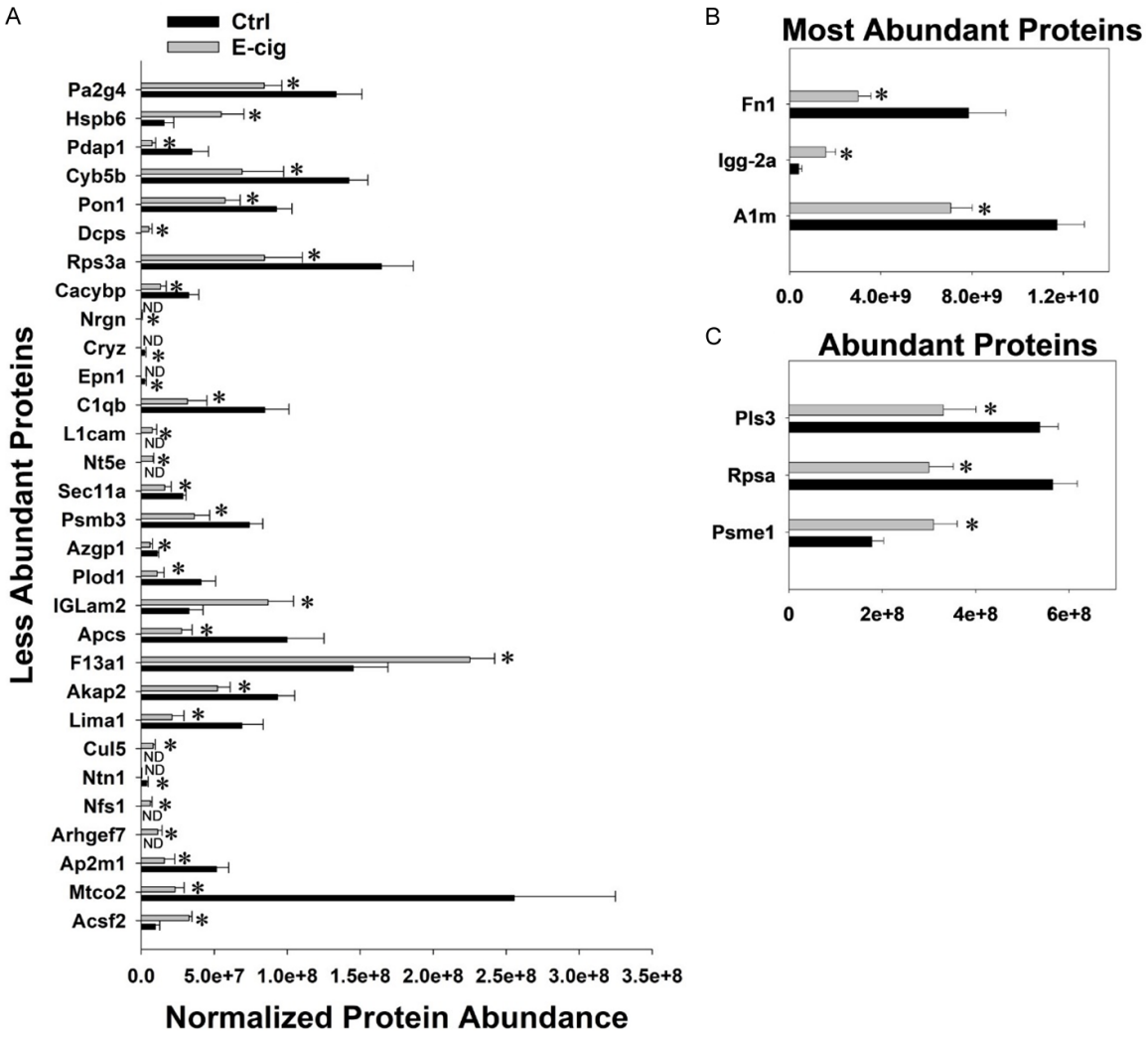

Figure 2. E-cig vaping during pregnancy alters protein signature in the uterine artery. Significantly altered proteins were identified using mass spectrometry analysis and proteomics following E-cig vaping in pregnancy. A. A total of 2129 proteins were detected by LC MS/MS, of which 37 were significantly enriched. Many of these significantly enriched proteins were related to the immune system followed by vascular function. Some proteins related to nicotine metabolism and cigarette exposure were not detected in the Controls, while they were detected in the uterine arteries of e-cig exposed dams. B and C. More abundant proteins in the uterine artery are depicted in a different scale. *, $P < 0.05$; ND, not detected.

closely associated with endothelial function, ribosomal protein SA (RPSA, P = 0.046), and proteasome activator complex subunit 1 (PSME1, P = 0.042) were altered. Many of the significantly altered proteins were directly related to the immune system (C1qb, IgG2a), followed by those related to uterine artery vasodilation. Proteins related to vasodilation included small heat shock protein 20 (HspB6, P = 0.049), cytochrome b5 reductase 3 (Cyb5b, P = 0.048), associated with vasodilatory nitric oxide signaling sensitization, paraoxonase 1 (Pon1, P = 0.046), and calcyclin-binding protein (Cacybp P = 0.045). Interestingly, some proteins were expressed only in the E-Cig group and were not expressed in the Controls; these included quinone oxidoreductase, related to e-cig metabolism (cryz), and netrin-1 (Ntn1), which is documented to significantly increase in smokers. Volcano plot mapping out the distribution of differentially expressed proteins in the maternal uterine artery following E-cig vaping in pregnancy is depicted in **Figure 3**. Gene ontology analyses confirmed these findings (**Figure 3**), showing that biological regulation and cellular processes were most altered followed by

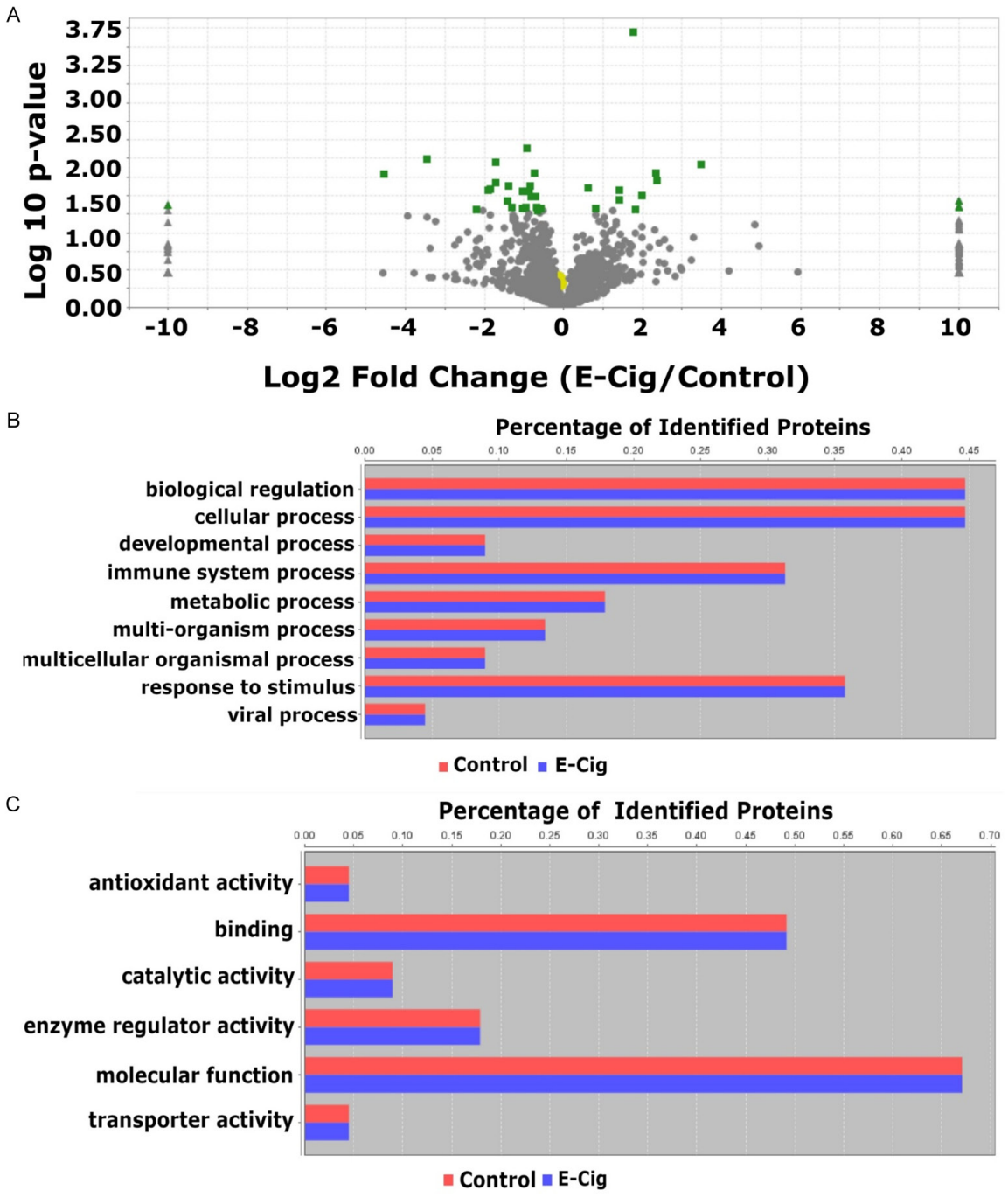

Figure 3. E-cig vaping during pregnancy protein signature in the uterine artery in pregnant rats. A. Volcano plot mapping out the distribution of differentially expressed proteins in the maternal uterine artery following E-cig vaping in pregnancy. Green dots indicate significantly altered proteins. B and C. The Gene Ontology terms of all the proteins that were significantly altered by e-cig, except for the unidentified protein, were classified according to their associated biological and cellular processes.

immune system alteration and response to stimulus. Among altered cellular processes, the most enriched proteins were related to protein binding and molecular function followed by enzymatic activity. We followed these studies with a machine learning based analyses of proteomic data and physiologic studies on uterine artery function. Based on cumulative explained variance for significantly altered proteins, 2 PCA components were enough to explain more

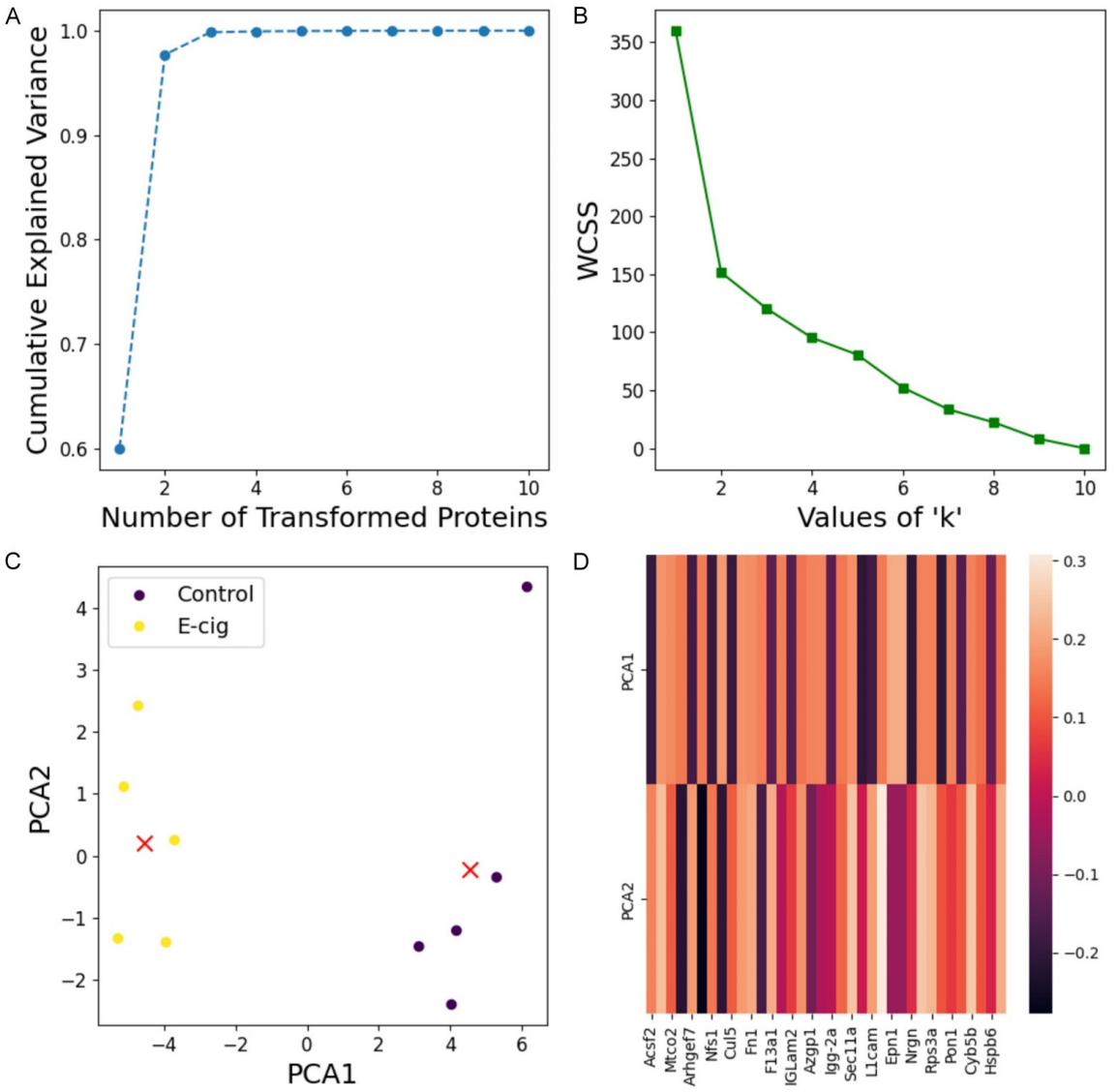

Figure 4. Validation for protein signature. A. The significant difference between the control and E-cig groups were validated using principal component analysis (PCA) and k-means clustering method. B. Feature transformation for significantly enriched proteins was performed by PCA, and then the transformed features were used in k-means clustering. C. The clusters using the transformed PCA components shows a clear distinction between control and E-cig groups. D. The heatmap denotes the contribution of each significantly enriched protein with reference to the PCA component.

than 95% of variances from Control and E-cig observations. The two PCA components were used for each observation of E-cig and Control groups to estimate parameter 'k' using WCSS. The PCA components for Control and E-cig groups are as follows: [3.12, -1.46] [4.17, -1.20] [6.14, 4.33] [4.03, -2.39] [5.29, -0.34] [-5.28, -1.33] [-3.70, 0.25] [-5.12, 1.11] [-3.94, -1.39] [-4.72, 2.42]. The elbow method and WCSS validated the two clusters. The centroids of clusters were calculated as [4.55, -0.21] and [-4.55, 0.21] for two-dimensional PCA components, and transformed significantly altered proteins clustered around the centroids. The clusters clearly depicted the distinction between Control and E-cig groups (**Figure 4**).

E-cig vaping significantly decreased uterine artery functional response in a pressurized vessel

Figure 5 depicts a comparative illustration of dose-dependent vasodilatory response. Maximal percent relaxation of the maternal uterine

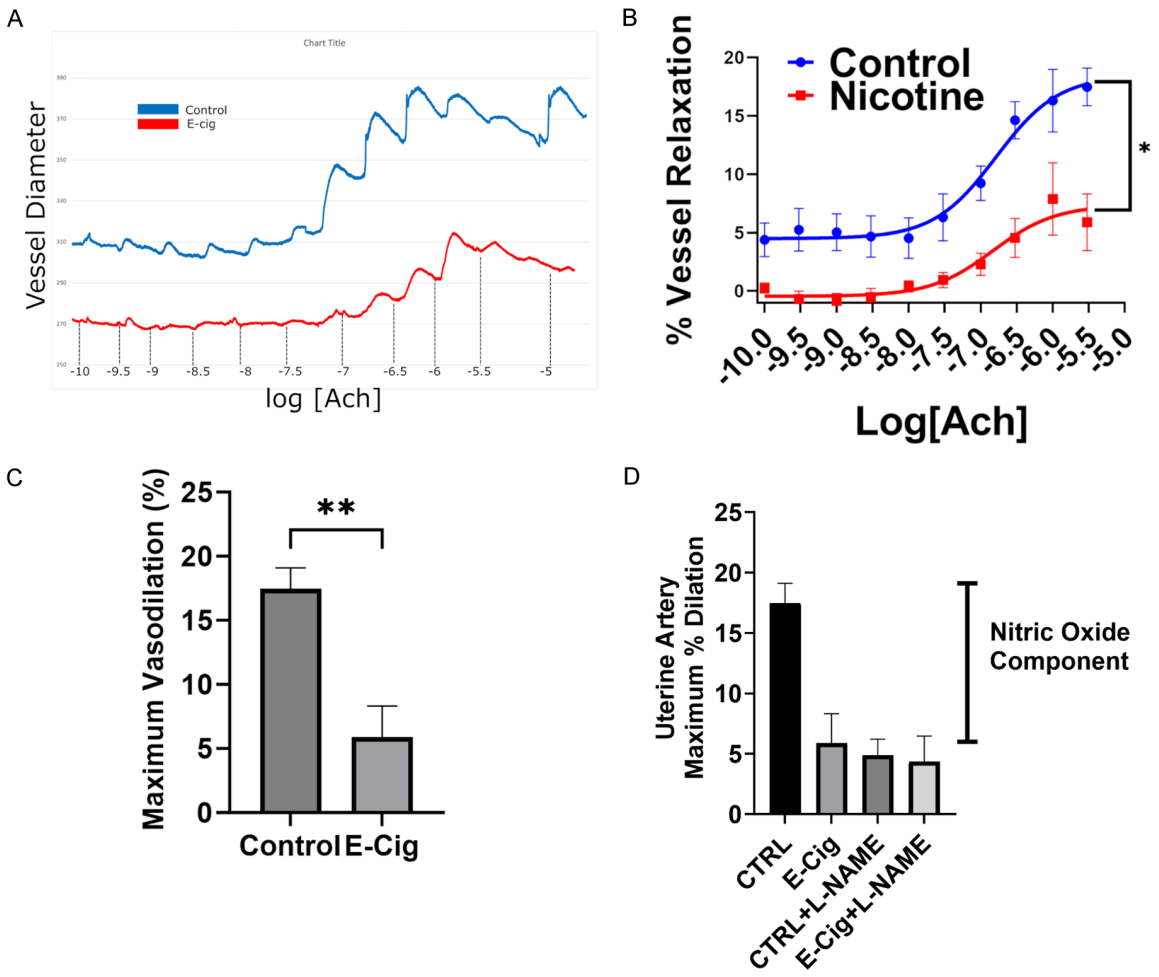

Figure 5. E-cig vaping during pregnancy attenuates NO-mediated vasodilation of the uterine artery. (A) Concentration-dependent vasodilatory effect on uterine arteries of the e-cig exposed rats, with (B) vessel relaxation improved ($P < 0.0001$) with Ach, but a significant treatment effect vasodilatory deficit ($P = 0.0010$). (C) Maximal Ach-induced uterine artery relaxation was impaired in uterine arteries of e-cig exposed rats (Control vs. E-Cig, ↓69.5%). (D) Supplementation of the NO inhibitor L-NAME decreased the uterine artery vasodilation in both control and e-cig. In the absence of L-NAME, the E-Cig group exhibited significantly lower maximum dilation compared to the Controls ($P = 0.001$). With the addition of L-NAME, the Control group exhibited significantly lower maximal dilation compared to the Controls without L-NAME ($P < 0.01$). In contrast, with the addition of L-NAME, the E-Cig group exhibited no difference compared to E-Cig group without L-NAME ($P = 0.706$) and the decrease in maximal Ach-induced vasodilation in the E-Cig groups could be entirely attributed to the NO component in the primary uterine artery. ** represents significant difference ($P < 0.05$) compared to the controls.

artery with increasing Ach dose administration was significantly lower in the E-Cig group compared with that in the pair-fed Control group (**Figure 5**). Pair-wise comparisons showed a concentration-dependent vasodilatory effect on uterine arteries of the e-cig exposed rats, with vessel relaxation improved ($P < 0.0001$) by Ach, but a significant treatment effect ($P = 0.0010$). E-cig exposed rats exhibited significant deficit in uterine artery relaxation; maximal Ach-induced uterine artery relaxation was impaired in uterine arteries of e-cig exposed rats (Ach [1e-5 M] Control vs. E-cig, ↓69.5%) (**Figure 5**). We then shortlisted the nitric oxide system to investigate its role in Ach-induced vasodilation as a number of proteins related to this vasodilatory system were detected in the uterine artery.

E-cig vaping specifically altered NO-mediated uterine artery functional response

Supplementation of the NO inhibitor L-NAME decreased the uterine artery vasodilation in

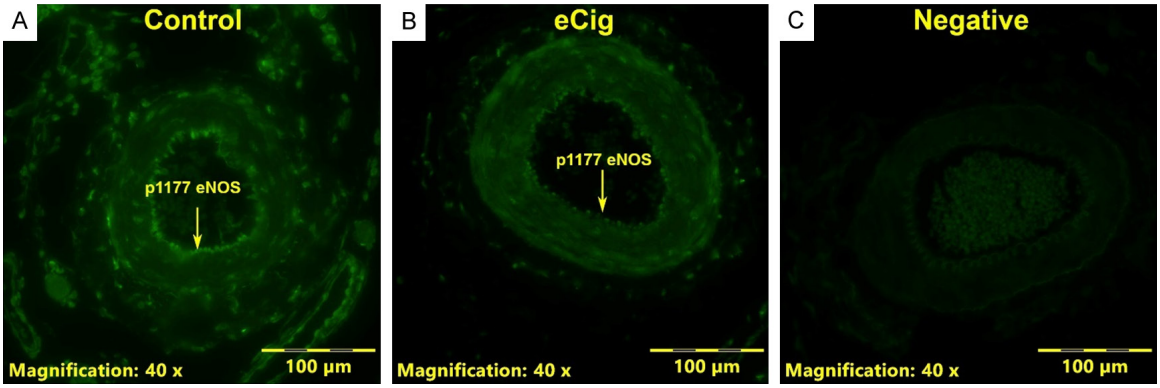

Figure 6. Immunohistochemistry analysis of P-Ser^{1177}eNOS levels in the primary uterine artery. Immunofluorescence staining demonstrates a localized expression of P-Ser^{1177}eNOS in the endothelium in both the (A) pair-fed control and (B) e-cig exposed rat with a major decrease of excitatory P-Ser^{1177}eNOS level in the uterine artery of the e-cig exposed rat compared to expression in the pair-fed control. (C) Negative control immunofluorescence image from a pregnant rat uterine artery.

both Control and E-Cig groups (**Figure 5**). In the absence of L-NAME, the E-Cig group exhibited significantly lower maximum dilation compared to the Controls ($P = 0.001$). With the addition of L-NAME, the Control group exhibited significantly lower maximal dilation compared to the Controls without L-NAME ($P < 0.01$). In contrast, with the addition of L-NAME, the E-Cig group exhibited no difference compared to E-Cig group without L-NAME ($P = 0.706$) and the decrease in maximal Ach-induced vasodilation in the E-Cig groups could be entirely attributed to the NO component in the primary uterine artery.

E-cig vaping significantly altered excitatory Ser^{1177}eNOS system

Uterine artery sections isolated from pair-fed Control and E-Cig rats were probed with a P-Ser^{1177}eNOS. Immunofluorescence imaging (**Figure 6**) demonstrated that eNOS was detected exclusively in the uterine artery endothelial cells. The level of florescence showed major decreases in the levels of phosphorylation at the Ser^{1177}eNOS between the control and E-Cig groups.

Discussion

This is the first study to demonstrate *in vivo* that e-cig aerosol exposure during pregnancy disrupts the uterine artery proteome and related vascular function (**Figure 7**).

Nicotine and the maternofetal unit

In vivo, non-pregnant human arteries and veins have impaired NO-mediated endothelium-dependent relaxation when exposed to tobacco smoking [29] and nicotine infusion [30]. Protein free nicotine and cotinine rapidly cross the placenta [31] via passive diffusion, as well as via efflux [31] and influx transporters due to their low molecular weight and high lipid solubility. Nicotine is a substrate for organic cation transporters nicotinic acetylcholine receptors (nAChRs), which are abundantly expressed in the placenta [32]. Nicotine then equilibrates in the fetal serum and amniotic fluid at concentrations equivalent to or higher than maternal serum levels [33]. Nicotine smoking causes oxidative stress, leading to abnormal placental vasculature development via transcriptome alterations [34] that limit the ability of the placenta to modulate the toxic effects. The concentration of nAChRs expressed in the placenta are altered by nicotine exposure [35]; however, with differing expression of nAChR subunits between nicotine exposed and unexposed placentas [36]. Histologic evidence of nicotine's effects on the placenta is demonstrated as increases in syncytial knots, syncytiotrophoblast necrosis, decreases in vascularization, vasculosyncytial membrane and cytotrophoblast proliferation [37, 38]. These acquired defects are known to cause placental insufficiency [38], leading to adverse pregnancy outcomes including spontaneous abortion, premature rupture of membranes, spontane-

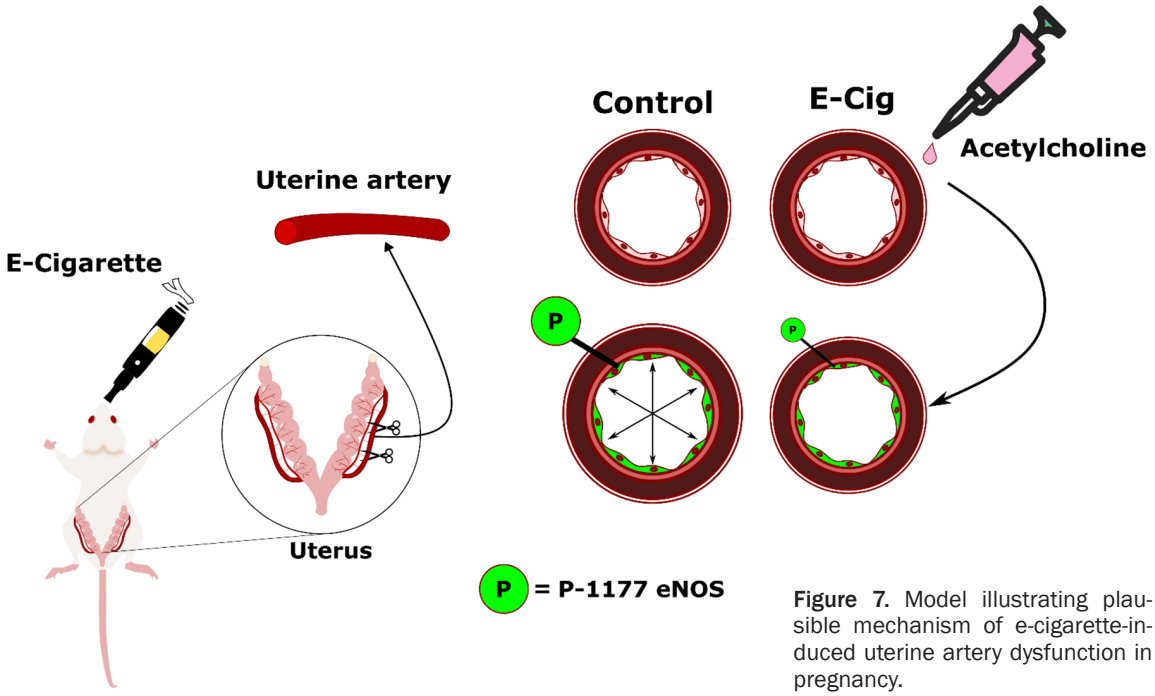

Figure 7. Model illustrating plausible mechanism of e-cigarette-induced uterine artery dysfunction in pregnancy.

ous preterm birth, FGR, sudden infant death syndrome (SIDS), and perinatal mortality [14].

Aerosolization of a nicotine containing liquid is fundamentally different than combustion of dried tobacco

In the process of aerosolization, free radicals and toxic byproducts are created due to: (1) chamber temperature, (2) coil metal composition, and (3) propylene glycol (PG): vegetable glycerin (VG) ratio. The power of the e-cigarettes affects the toxicant production with increasing power leading to higher generated temperatures and the creation of more aerosolized toxicants [39]. The temperatures required for e-cigs to vaporize the basic chemical constituents in e-liquids (carrier liquids PG, VG, and nicotine) are higher than temperatures required for traditional tobacco products. The temperature of the combustion zone in a tobacco pipe is around 500°C (variability, 380°-620°C) and in cigarettes averages 650°C (variability, 470°-812°C) [40]. Unlike the traditional method of burning dried tobacco, the vaporization temperature of e-cigs relies on heating combinations of iron, chromium, and nickel chromium wires. Over time, heat cycles cause coil metal loss, which potentially enters the inhaled aerosol plume [41]. Infrared temperature sensors found that both 100% PG and 100% VG saturated coils averaged below 300°C [41]. When e-cigarettes were activated without a liquid in the chamber, the temperatures generated by the e-cig coils reached as high as 1000°C [41]. The temperature within the chamber becomes an issue with regard to common practices regarding e-cigarettes. E-cig users report dry activation of the devices as a method of "cleaning" [41] the liquid chamber, thereby reaching temperatures unobtainable when filled with vape juice and nicotine, and producing toxic byproducts [18, 42, 43].

Proteomic analyses and use of machine learning in the gestational e-cig field

We are not aware of any proteomic studies in pregnancy following e-cig vaping. However, a few proteomic studies following e-cig exposure exist outside pregnancy. *In vitro* exposure to e-cig liquids show significant depletion in total number of proteins and impairment of mitochondrial function in treated V79 cells [44]. Urine collected from a rat e-cig model before and after two weeks of e-cig vaping showed altered proteins related to lung function, metabolic pathways and cardiovascular function [45]. Another proteomic analysis on 16HBE cells *in vitro* identified 431 differentially expressed exosomal proteins and that traditional cigarette had a greater impact than e-cigs on

exosomal protein expression [46]. From a physiologic perspective, proteomic analyses showed that many of the significantly altered proteins were directly related to the immune system followed by those related to uterine artery vasodilation. From both a metabolic and biomarker perspective, proteomic analyses detected proteins that were expressed only after e-cig vaping. These included those directly related to nicotine metabolism and markers of nicotine exposure in traditional cigarette smoking. Our data demonstrate and also effectively make use of the advances in the field of quantitative mass spectrometry to detect extremely subtle plasma protein alterations associated with maternal e-cig use. These data were further validated by principal component analyses and clustering methods.

Clinical implications

In vivo effects of e-cig vaping: Our group previously published [18], non-invasive, *in vivo*, hemodynamic measurements of the rat maternal uterine artery and the fetal umbilical artery were interrogated in both B-mode and color pulse wave Doppler to obtain measurement parameters. Our study found a marked decrease in blood velocimetry in both the maternal uterine and fetal umbilical circulation, with a non-significant decrease after e-cig juice exposure alone, and a progressive decrease in blood velocimetry after combined e-cig juice and nicotine exposure [18]. Oxygen diffusion from mother to fetus across the placenta is primarily dependent on the uterine artery blood flow rate [47], therefore, a decrease in placental perfusion can be extrapolated to lead to decreased oxygenation of the fetoplacental unit. This current study used direct measurement of the uterine artery vasodilation under physiologic conditions and the results paralleled our previously published indirect ultrasonographic Doppler evaluation of uterine artery Doppler velocimetry compromise in e-cig exposed dams [18]. The maternofetal unit relies on adequate vascular perfusion for optimal metabolism and fetal and placental growth. Animal models [18] and our current study demonstrate the detrimental effects of e-cig aerosol vaping on prenatal development. This current study shows that vaping e-cigs containing nicotine leads to a FGR phenotype [48] of decreased fetal weight, CRL, and placental weight, which is consistent with our previous study [18]. The current study adds a possible mechanistic cause to the FGR phenotype: disruption of the uterine artery vasodilatory endothelial nitric oxide synthase (eNOS) pathway. Rat prenatal e-cig exposure is known to dysregulate fetal lung gene expression [49], to inhibit alveolar cell proliferation and postnatal lung development [50], alter gene expression in the frontal cortex [24] of the brain, and result in localized inflammation of the hippocampus [51]. Further research is required to determine the upstream pathway(s) that are altered by e-cig exposure in utero.

Endothelial nitric oxide synthase (eNOS) and vasodilation of the uterine artery: Nitric oxide (NO) is a cellular signaling molecule that modulates insulin secretion, peristalsis, and airway and vascular tone and is a powerful vasodilator. While there are several regulatory systems of eNOS function, eNOS-Ser^{1177} phosphorylation is a major regulator of eNOS activity [52, 53]. The effects of traditional maternal prenatal tobacco smoking are well known and include: a reduction in eNOS levels in the fetal circulation [12], decreased eNOS activity in fetal umbilical veins [12], and reduced serum eNOS concentration in newborns [12], when compared to nonsmokers. Decreased eNOS expression in the umbilical artery (UA) [54, 55] is found in pregnancies complicated by FGR, and pregnancies of non-smokers complicated by preeclampsia and FGR have higher plasma concentrations of asymmetric dimethylarginine (ADMA) [56], an endogenous inhibitor of eNOS that competes with L-arginine, and lower activity of eNOS in placental villous tissue [57]. While studies examining e-cigarette effects on uterine artery are limited, Anderson et al., 2011 examined human myometrial biopsies obtained during elective cesarean deliveries of nonsmokers, former smokers, and active smokers *in vitro* using wire myograph [58]. Wire myograph indirectly measured vasoconstrictor response as well as endothelium-dependent relaxation between the groups using the vasodilators bradykinin and the nitric oxide donor sodium nitroprusside, respectively [58]. Immunohistochemical (IHC) characterization of placental nitric oxide synthase expression in preeclampsia compared to normotensive pregnancies found that the syncytiotrophoblast had a primarily basal and punctate distribution in nor-

motensive patients, but a primarily apical and diffuse IHC distribution in preeclamptic patients [59]. Ghabour et al. hypothesized that relative hypoxia of the fetal-placental unit may lead to smooth muscle proliferation and altered expression of endothelial nitric oxide synthase in the terminal villous vessels. In a similar fashion, we found decreased P-Ser^{1177}eNOS IHC staining of the endothelium of the uterine artery in e-cig exposed dams, but not in the unexposed dams. Our current research has established the basis for further investigation exploring the mechanistic pathways that dysregulate this physiologic process. The next steps will be to further delineate the pathway(s) involved, and potentially identify specific mechanistic targets that could prevent e-cig-induced vasodilatory defects.

Research implications

Further research is needed to identify the molecular pathways and mechanisms by which e-cig aerosols cause uterine artery dysfunction, and thereby, identify therapeutic targets to prevent, reduce, and/or reverse e-cig mediated uteroplacental dysfunction and FGR. Additionally, it is important to perform studies on the myriad e-cig liquid flavorings in order to elucidate their potential impact(s) on the maternofetal unit. This will allow for a more comprehensive understanding of the public health risks and creation of regulatory measures regarding flavoring components and manufacturing.

Acknowledgements

This work was supported by the National Institutes of Health, USA [AA23035 (JR), AA23520 (JR), HL151497 (JR), ES036084].

Disclosure of conflict of interest

None.

Abbreviations

Ach, Acetylcholine; °C, Degree celsius; Control, Pair-fed control; CRL, Crown-rump length; E-cig(s), Electronic cigarette(s); ENDS, Electronic nicotine delivery systems; eNOS, Endothelial nitric oxide synthase; FGR, Fetal growth restriction; GD, Gestational day; Hr, Hour; Juice, Vegetable glycerin (VG) + Propylene glycerol (PG); LBW, Low birth weight; Mins, Minutes; nAChR, Nicotinic acetylcholine receptor; Nicotine, Pair-fed Juice + Nicotine; NO, Nitric oxide; NOS, Nitric oxide synthase; PBS, Phosphate-buffered saline; PG, Propylene glycol; PND, Postnatal day; PTB, Preterm birth; SGA, Small-for-gestational age; TBX, Thromboxane; UA, Uterine artery; VG, Vegetable glycerin.

Address correspondence to: Dr. Jayanth Ramadoss, Department of Obstetrics and Gynecology and Department of Physiology, School of Medicine, Wayne State University, 275 E Hancock Street, C.S. Mott Center for Human Growth and Development, Rm 195, Detroit, MI 48201, USA. Tel: 313-577-7818; E-mail: hh1065@wayne.edu

References

[1] National Center for Chronic Disease Prevention and Health Promotion (US) Office on Smoking and Health. The Health Consequences of Smoking-50 Years of Progress: A Report of the Surgeon General. Atlanta (GA): Centers for Disease Control and Prevention (US); 2014.

[2] Dutra LM and Glantz SA. E-cigarettes and national adolescent cigarette use: 2004-2014. Pediatrics 2017; 139: e20162450.

[3] Duke JC, Allen JA, Eggers ME, Nonnemaker J and Farrelly MC. Exploring differences in youth perceptions of the effectiveness of electronic cigarette television advertisements. Nicotine Tob Res 2016; 18: 1382-1386.

[4] Anand V, McGinty KL, O'Brien K, Guenthner G, Hahn E and Martin CA. E-cigarette use and beliefs among urban public high school students in north carolina. J Adolesc Health 2015; 57: 46-51.

[5] Lyu JC, Huang P, Jiang N and Ling PM. A systematic review of e-cigarette marketing communication: messages, communication channels, and strategies. Int J Environ Res Public Health 2022; 19: 9263.

[6] Wang TW, Gentzke AS, Creamer MR, Cullen KA, Holder-Hayes E, Sawdey MD, Anic GM, Portnoy DB, Hu S, Homa DM, Jamal A and Neff LJ. Tobacco product use and associated factors among middle and high school students - united states, 2019. MMWR Surveill Summ 2019; 68: 1-22.

[7] Zaganjor I, Kramer RD, Kofie JN, Sawdey MD and Cullen KA. Trends in smoking before, during, and after pregnancy in the united states from 2000 to 2020: pregnancy risk assessment monitoring system. J Womens Health (Larchmt) 2023; 33: 283-293.

[8] Tong VT, Dietz PM, Morrow B, D'Angelo DV, Farr SL, Rockhill KM and England LJ; Centers for

Disease Control and Prevention (CDC). Trends in smoking before, during, and after pregnancy--pregnancy risk assessment monitoring system, united states, 40 sites, 2000-2010. MMWR Surveill Summ 2013; 62: 1-19.
[9] Wagner NJ, Camerota M and Propper C. Prevalence and perceptions of electronic cigarette use during pregnancy. Matern Child Health J 2017; 21: 1655-1661.
[10] Simpson WJ. A preliminary report on cigarette smoking and the incidence of prematurity. Am J Obstet Gynecol 1957; 73: 807-815.
[11] Xu R, Hong X, Zhang B, Huang W, Hou W, Wang G, Wang X, Igusa T, Liang L and Ji H. DNA methylation mediates the effect of maternal smoking on offspring birthweight: a birth cohort study of multi-ethnic US mother-newborn pairs. Clin Epigenetics 2021; 13: 47.
[12] Andersen MR, Walker LR and Stender S. Reduced endothelial nitric oxide synthase activity and concentration in fetal umbilical veins from maternal cigarette smokers. Am J Obstet Gynecol 2004; 191: 346-351.
[13] Wang X, Zuckerman B, Pearson C, Kaufman G, Chen C, Wang G, Niu T, Wise PH, Bauchner H and Xu X. Maternal cigarette smoking, metabolic gene polymorphism, and infant birth weight. JAMA 2002; 287: 195-202.
[14] Holloway AC, Salomon A, Soares MJ, Garnier V, Raha S, Sergent F, Nicholson CJ, Feige JJ, Benharouga M and Alfaidy N. Characterization of the adverse effects of nicotine on placental development: in vivo and in vitro studies. Am J Physiol Endocrinol Metab 2014; 306: E443-456.
[15] Kim S and Oancea SC. Electronic cigarettes may not be a "safer alternative" of conventional cigarettes during pregnancy: evidence from the nationally representative PRAMS data. BMC Pregnancy Childbirth 2020; 20: 557.
[16] Cardenas VM, Cen R, Clemens MM, Moody HL, Ekanem US, Policherla A, Fischbach LA, Eswaran H, Magann EF and Delongchamp RR. Use of electronic nicotine delivery systems (ENDS) by pregnant women I: risk of small-for-gestational-age birth. Tob Induc Dis 2019; 17: 44.
[17] Papageorghiou AT, Christina K and Nicolaides KH. The role of uterine artery doppler in predicting adverse pregnancy outcome. Best Pract Res Clin Obstet Gynaecol 2004; 18: 383-396.
[18] Orzabal MR, Lunde-Young ER, Ramirez JI, Howe SY, Naik VD, Lee J, Heaps CL, Threadgill DW and Ramadoss J. Chronic exposure to e-cig aerosols during early development causes vascular dysfunction and offspring growth deficits. Transl Res 2019; 207: 70-82.
[19] Naik VD, Davis-Anderson K, Subramanian K, Lunde-Young R, Nemec MJ and Ramadoss J. Mechanisms underlying chronic binge alcohol exposure-induced uterine artery dysfunction in pregnant rat. Alcohol Clin Exp Res 2018; 42: 682-690.
[20] Hahn J, Monakhova YB, Hengen J, Kohl-Himmelseher M, Schüssler J, Hahn H, Kuballa T and Lachenmeier DW. Electronic cigarettes: overview of chemical composition and exposure estimation. Tob Induc Dis 2014; 12: 23.
[21] Son Y, Wackowski O, Weisel C, Schwander S, Mainelis G, Delnevo C and Meng Q. Evaluation of e-vapor nicotine and nicotyrine concentrations under various e-liquid compositions, device settings, and vaping topographies. Chem Res Toxicol 2018; 31: 861-868.
[22] Goniewicz ML, Kuma T, Gawron M, Knysak J and Kosmider L. Nicotine levels in electronic cigarettes. Nicotine Tob Res 2012; 15: 158-166.
[23] Matta SG, Balfour DJ, Benowitz NL, Boyd RT, Buccafusco JJ, Caggiula AR, Craig CR, Collins AC, Damaj MI, Donny EC, Gardiner PS, Grady SR, Heberlein U, Leonard SS, Levin ED, Lukas RJ, Markou A, Marks MJ, McCallum SE, Parameswaran N, Perkins KA, Picciotto MR, Quik M, Rose JE, Rothenfluh A, Schafer WR, Stolerman IP, Tyndale RF, Wehner JM and Zirger JM. Guidelines on nicotine dose selection for in vivo research. Psychopharmacology (Berl) 2007; 190: 269-319.
[24] Lauterstein DE, Tijerina PB, Corbett K, Akgol Oksuz B, Shen SS, Gordon T, Klein CB and Zelikoff JT. Frontal cortex transcriptome analysis of mice exposed to electronic cigarettes during early life stages. Int J Environ Res Public Health 2016; 13: 417.
[25] Naik VD, Lunde-Young ER, Davis-Anderson KL, Orzabal M, Ivanov I and Ramadoss J. Chronic binge alcohol consumption during pregnancy alters rat maternal uterine artery pressure response. Alcohol 2016; 56: 59-64.
[26] Subramanian K, Naik VD, Sathishkumar K, Yallampalli C, Saade GR, Hankins GD and Ramadoss J. Chronic binge alcohol exposure during pregnancy impairs rat maternal uterine vascular function. Alcohol Clin Exp Res 2014; 38: 1832-1838.
[27] Chinnathambi V, Balakrishnan M, Ramadoss J, Yallampalli C and Sathishkumar K. Testosterone alters maternal vascular adaptations: role of the endothelial NO system. Hypertension 2013; 61: 647-654.
[28] Angiolini E, Fowden A, Coan P, Sandovici I, Smith P, Dean W, Burton G, Tycko B, Reik W and Sibley C. Regulation of placental efficiency for nutrient transport by imprinted genes. Placenta 2006; 27: 98-102.

[29] Ueda S, Matsuoka H, Miyazaki H, Usui M, Okuda S and Imaizumi T. Tetrahydrobiopterin restores endothelial function in long-term smokers. J Am Coll Cardiol 2000; 35: 71-75.
[30] Chalon S, Moreno H Jr, Benowitz NL, Hoffman BB and Blaschke TF. Nicotine impairs endothelium-dependent dilatation in human veins in vivo. Clin Pharmacol Ther 2000; 67: 391-397.
[31] Lin IH, Yang L, Dalley JW and Tsai TH. Transplacental transfer of nicotine: modulation by organic cation transporters. Biomed Pharmacother 2022; 145: 112489.
[32] Sata R, Ohtani H, Tsujimoto M, Murakami H, Koyabu N, Nakamura T, Uchiumi T, Kuwano M, Nagata H and Tsukimori K. Functional analysis of organic cation transporter 3 expressed in human placenta. J Pharmacol Exp Ther 2005; 315: 888-895.
[33] Luck W, Nau H, Hansen R and Steldinger R. Extent of nicotine and cotinine transfer to the human fetus, placenta and amniotic fluid of smoking mothers. Dev Pharmacol Ther 1985; 8: 384-395.
[34] Votavova H, Dostalova Merkerova M, Fejglova K, Vasikova A, Krejcik Z, Pastorkova A, Tabashidze N, Topinka J, Veleminsky M Jr, Sram RJ and Brdicka R. Transcriptome alterations in maternal and fetal cells induced by tobacco smoke. Placenta 2011; 32: 763-770.
[35] Makowski EL, Meschia G, Droegemueller W and Battaglia FC. Distribution of uterine blood flow in the pregnant sheep. Am J Obstet Gynecol 1968; 101: 409-412.
[36] Machaalani R, Ghazavi E, Hinton T, Waters KA and Hennessy A. Cigarette smoking during pregnancy regulates the expression of specific nicotinic acetylcholine receptor (nAChR) subunits in the human placenta. Toxicol Appl Pharmacol 2014; 276: 204-212.
[37] Sbrana E, Suter MA, Abramovici AR, Hawkins HK, Moss JE, Patterson L, Shope C and Aagaard-Tillery K. Maternal tobacco use is associated with increased markers of oxidative stress in the placenta. Am J Obstet Gynecol 2011; 205: 246, e241-247.
[38] Pintican D, Poienar AA, Strilciuc S and Mihu D. Effects of maternal smoking on human placental vascularization: a systematic review. Taiwan J Obstet Gynecol 2019; 58: 454-459.
[39] Wagener TL, Floyd EL, Stepanov I, Driskill LM, Frank SG, Meier E, Leavens EL, Tackett AP, Molina N and Queimado L. Have combustible cigarettes met their match? The nicotine delivery profiles and harmful constituent exposures of second-generation and third-generation electronic cigarette users. Tob Control 2017; 26: e23-e28.
[40] ERMALA P and HOLSTI LR. On the burning temperatures of tobacco. Cancer Res 1956; 16: 490-495.
[41] Mulder HA, Stewart JB, Blue IP, Krakowiak RI, Patterson JL, Karin KN, Royals JM, DuPont AC, Forsythe KE, Poklis JL, Poklis A, Butler SN, Turner JBM and Peace MR. Characterization of E-cigarette coil temperature and toxic metal analysis by infrared temperature sensing and scanning electron microscopy - energy-dispersive X-ray. Inhal Toxicol 2020; 32: 447-455.
[42] Bitzer ZT, Goel R, Reilly SM, Foulds J, Muscat J, Elias RJ and Richie JP Jr. Effects of solvent and temperature on free radical formation in electronic cigarette aerosols. Chem Res Toxicol 2018; 31: 4-12.
[43] Gillman IG, Kistler KA, Stewart EW and Paolantonio AR. Effect of variable power levels on the yield of total aerosol mass and formation of aldehydes in e-cigarette aerosols. Regul Toxicol Pharmacol 2016; 75: 58-65.
[44] Trifunovic S, Smiljanić K, Sickmann A, Solari FA, Kolarevic S, Divac Rankov A and Ljujic M. Electronic cigarette liquids impair metabolic cooperation and alter proteomic profiles in V79 cells. Respir Res 2022; 23: 191.
[45] Liu Y, Shen Z, Zhao C and Gao Y. Urine proteomic analysis of the rat e-cigarette model. PeerJ 2023; 11: e16041.
[46] Wang W, Zeng R, Liu M, Chen M, Wei S, Li B and Yu S. Exosome proteomics study of the effects of traditional cigarettes and electronic cigarettes on human bronchial epithelial cells. Toxicology in Vitro 2023; 86: 105516.
[47] Parer JT, Del Lannoy CW, Hoversland AS and Metcalfe J. Effect of decreased uterine blood flow on uterine oxygen consumption in pregnant macaques. Am J Obstet Gynecol 1968; 100: 813-820.
[48] Holemans K, Aerts L and Van Assche FA. Fetal growth and long-term consequences in animal models of growth retardation. Eur J Obstet Gynecol Reprod Biol 1998; 81: 149-156.
[49] Chen H, Li G, Chan YL, Chapman DG, Sukjamnong S, Nguyen T, Annissa T, McGrath KC, Sharma P and Oliver BG. Maternal E-cigarette exposure in mice alters DNA methylation and lung cytokine expression in offspring. Am J Respir Cell Mol Biol 2018; 58: 366-377.
[50] McGrath-Morrow SA, Hayashi M, Aherrera A, Lopez A, Malinina A, Collaco JM, Neptune E, Klein JD, Winickoff JP, Breysse P, Lazarus P and Chen G. The effects of electronic cigarette emissions on systemic cotinine levels, weight and postnatal lung growth in neonatal mice. PLoS One 2015; 10: e0118344.
[51] Zelikoff JT, Parmalee NL, Corbett K, Gordon T, Klein CB and Aschner M. Microglia activation and gene expression alteration of neurotrophins in the hippocampus following early-life exposure to E-cigarette aerosols in a murine model. Toxicol Sci 2018; 162: 276-286.

[52] Fulton D, Gratton JP, McCabe TJ, Fontana J, Fujio Y, Walsh K, Franke TF, Papapetropoulos A and Sessa WC. Regulation of endothelium-derived nitric oxide production by the protein kinase Akt. Nature 1999; 399: 597-601.
[53] Dimmeler S, Fleming I, Fisslthaler B, Hermann C, Busse R and Zeiher AM. Activation of nitric oxide synthase in endothelial cells by Akt-dependent phosphorylation. Nature 1999; 399: 601-605.
[54] Suzuki K, Minei LJ and Johnson EE. Effect of nicotine upon uterine blood flow in the pregnant rhesus monkey. Am J Obstet Gynecol 1980; 136: 1009-1013.
[55] Rutherford RA, McCarthy A, Sullivan MH, Elder MG, Polak JM and Wharton J. Nitric oxide synthase in human placenta and umbilical cord from normal, intrauterine growth-retarded and pre-eclamptic pregnancies. Br J Pharmacol 1995; 116: 3099-3109.
[56] Savvidou MD, Hingorani AD, Tsikas D, Frolich JC, Vallance P and Nicolaides KH. Endothelial dysfunction and raised plasma concentrations of asymmetric dimethylarginine in pregnant women who subsequently develop pre-eclampsia. Lancet 2003; 361: 1511-1517.
[57] Morris NH, Sooranna SR, Learmont JG, Poston L, Ramsey B, Pearson JD and Steer PJ. Nitric oxide synthase activities in placental tissue from normotensive, pre-eclamptic and growth retarded pregnancies. Br J Obstet Gynaecol 1995; 102: 711-714.
[58] Andersen MR, Uldbjerg N, Stender S, Sandager P and Aalkjær C. Maternal smoking and impaired endothelium-dependent nitric oxide-mediated relaxation of uterine small arteries in vitro. Am J Obstet Gynecol 2011; 204: 177.e171-177.e177.
[59] Ghabour MS, Eis AL, Brockman DE, Pollock JS and Myatt L. Immunohistochemical characterization of placental nitric oxide synthase expression in preeclampsia. Am J Obstet Gynecol 1995; 173: 687-694.